Structural and Functional Assessment of mBjAMP1, an Antimicrobial Peptide from *Branchiostoma japonicum*, Revealed a Novel α-Hairpinin-like Scaffold with Membrane Permeable and DNA Binding Activity

Jiyoung Nam,[†,‖] Hyosuk Yun,[†] Ganesan Rajasekaran,[‡] S. Dinesh Kumar,[‡] Jae Il Kim,[§] Hye Jung Min,[⊥] Song Yub Shin,*[,‡] and Chul Won Lee*[,†]

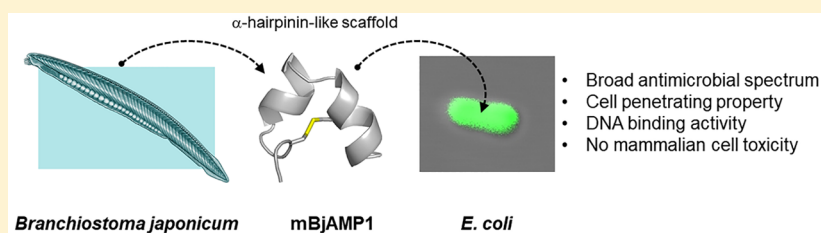[†]Department of Chemistry, Chonnam National University, Gwangju 61186, Republic of Korea

[‡]Department of Medical Science, Graduate School, and Department of Cellular and Molecular Medicine, School of Medicine, Chosun University, Gwangju 61452, Republic of Korea

[§]Department of Life Science, Gwangju Institute of Science and Technology, Gwangju 61005, Republic of Korea

[‖]Natural Constituents Research Center, Korea Institute of Science and Technology (KIST), Gangneung 25451, Republic of Korea

[⊥]Department of Cosmetic Science, Kwangju Women's University, Gwangju 62396, Republic of Korea

S Supporting Information

α-hairpinin-like scaffold

- Broad antimicrobial spectrum
- Cell penetrating property
- DNA binding activity
- No mammalian cell toxicity

Branchiostoma japonicum — mBjAMP1 — *E. coli*

ABSTRACT: Here we describe the three-dimensional structure and antimicrobial mechanism of mBjAMP1, an antimicrobial peptide (AMP) isolated from *Branchiostoma japonicum*. The structure of mBjAMP1 was determined by 2D solution NMR spectroscopy and revealed a novel α-hairpinin-like scaffold stabilized by an intramolecular disulfide bond. mBjAMP1 showed effective growth inhibition and bactericidal activities against pathogenic bacteria but was not cytotoxic to mammalian cells. Antimicrobial mechanism studies using fluorescence-based experiments demonstrated that mBjAMP1 did not disrupt membrane integrity. Laser-scanning confocal microscopy indicated that mBjAMP1 is able to penetrate the bacterial cell membrane without causing membrane disruption. Moreover, gel retardation assay suggested that mBjAMP1 directly binds to bacterial DNA as an intracellular target. Collectively, mBjAMP1 may inhibit biological functions by binding to DNA or RNA after penetrating the bacterial cell membrane, thereby causing cell death. These results suggest that mBjAMP1 may present a promising template for the development of peptide-based antibiotics.
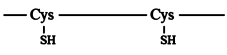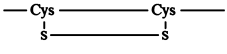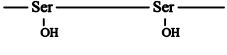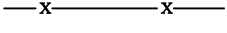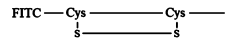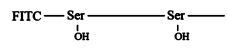
■ INTRODUCTION

The development of antibiotics, with new mechanisms of action, is urgently required due to the rapid increase in multidrug resistant (MDR) bacteria which pose a serious threat to public health.[1,2] Antimicrobial peptides (AMPs) are ubiquitous, naturally occurring molecules, which may also be produced by multicellular organisms to protect against pathogens.[3] AMPs are generally cationic peptides comprising less than 50 amino acids and display broad spectrum antimicrobial activity, which directly destroys various cell types, including bacteria and fungi, as well as viruses.[4] Furthermore, they play a crucial role in the innate immune system of higher organisms including plants and mammals.[5,6] In contrast to conventional antibiotics which block specific biosynthetic pathways such as protein or cell wall synthesis, the antimicrobial activity of most AMPs occurs through physical disruption of the microbial cell membrane, which induces leakage of intracellular components, leading to microbial cell death.[7] These properties have allowed AMPs to gain recognition as potential alternatives to conventional antibiotics. AMPs are generally characterized by a cationic amphipathic structure in biological membrane environments, where one surface is positively charged, while the other exhibits a significant proportion of hydrophobic surface.[4] The activity of AMPs to kill bacteria mainly depends on their ability to interact with cell membranes or cell walls. Cationic AMPs selectively interact with negatively charged membranes, which leads to physical disruption of the bacterial membrane.[8] Selectivity toward bacterial membranes by AMPs is largely due

Table 1. Amino Acid Sequences and Physicochemical Properties of mBjAMP1 and Its Analogs

Peptides	Primary structure[a]	Schematic diagram	Molecular mass [M+H]$^+$	
			Calculated	Observed[b]
mBjAMP1-re	H-NLCASLRARHTIPQCRKFGRR-NH$_2$	—Cys———Cys— (SH, SH)	2483.9	2483.9
mBjAMP1-ox	H-NLCASLRARHTIPQCRKFGRR-NH$_2$	—Cys———Cys— (S—S)	2481.9	2481.9
mBjAMP1-ser	H-NLSASLRARHTIPQSRKFGRR-NH$_2$	—Ser———Ser— (OH, OH)	2451.8	2452.3
mBjAMP1-del	H-NLASLRARHTIPQRKFGRR-NH$_2$	—X———X—	2277.7	2277.1
FITC-mBjAMP1-ox	FITC-NLCASLRARHTIPQCRKFGRR-NH$_2$	FITC—Cys———Cys— (S—S)	2983.7	2983.5
FITC-mBjAMP1-ser	FITC-NLSASLRARHTIPQSRKFGRR-NH$_2$	FITC—Ser———Ser— (OH, OH)	2953.6	2953.7

^{a}All peptides except the FITC-labeled peptides have a free NH$_2$ group at the N-terminus, and the C-terminuses of all peptides are amidated.
^{b}Molecular masses were determined by LC–MS.

to variances in membrane composition of different microbes and cell types.[9]

AMPs are grouped into four classes according to their structural characteristics: amphipathic α-helical, disulfide (SS) bonded β-sheet, extended, and loop-structured peptides.[10] The α-helical AMPs such as magainin and cecropin are well studied in their structure−activity relationships. These peptides are usually disordered in aqueous solution but form a helical structure in membrane mimic environments. Most of the known α-helical AMPs exert their antimicrobial activity by disrupting and destroying the biological equilibrium of the cell membranes through different mechanisms including barrel-stave, carpet-like, and toroidal pore model.[11] The β-sheet AMPs including α-, β-defensins and β-hairpin peptides are stabilized by several SS bonds and form unique 3D structures. Many β-sheet AMPs disrupt bacterial membranes to exhibit their antimicrobial activities.[12] The extended and loop-structured AMPs do not form any secondary structure in aqueous solution. These extended and loop-structured AMPs are predominantly rich in specific residues including Pro, Trp, Arg, and His. Among these AMPs, some of Pro/Arg-rich AMPs such as indolicidin, PR-39, Bac7, oncocin, and apidaecin kill bacteria by diverse mechanisms different from membrane perturbation.[13−17] These intracellular-acting AMPs enter the bacterial cells without membrane lysis and may interact with intracellular molecules (DNA, RNA, or proteins), impairing specific vital biochemical processes (e.g., replication, translation, or enzyme activities), thereby causing cell death.[13−17] In addition to these Pro/Arg-rich AMPs, α-helical buforin II is also known as an intracellular-acting AMP that binds to DNA and RNA.[18,19]

mBjAMP1 is a novel AMP from amphioxus *Branchiostoma japonicum* (*B. japonicum*).[20] The *Bjamp1* gene, isolated from *B. japonicum,* encodes a protein of 97 amino acids comprising an N-terminal signal sequence, followed by anionic and C-terminal cationic regions. The C-terminal cationic peptide sequence characterizes mature AMPs, termed mBjAMP1, consisting of 21 amino acids with a net charge of +6 and a low sequence similar to known AMPs, indicating that mBjAMP1 is likely a novel AMP. The mBjAMP1 peptide

effectively inhibited the growth of a broad spectrum of bacteria but displayed no cytotoxicity to mammalian cells, suggesting high cell selectivity. Therefore, mBjAMP1 may be considered as a novel type of AMP with a high bacterial membrane selectivity, which offers a promising template for the development of novel peptides. However, to date, neither the three-dimensional structure nor the detailed antimicrobial mechanism of mBjAMP1 has been described. We determined the three-dimensional structure of mBjAMP1 using 2D solution NMR spectroscopy, which revealed that mBjAMP1 is composed of two α-helices stabilized by a single intra-molecular SS bond. The overall structure of mBjAMP1 adopts a helix−turn−helix conformation resembling α-hairpinin scaffold, characterized by two paired α-helices connected by two SS bridges. To assess the structural and functional roles of the SS bond in mBjAMP1, various mBjAMP1 analogs without the SS bond were prepared and analyzed for antimicrobial activity and mechanism of action. These studies revealed that the SS bond may affect the overall conformation, even under aqueous conditions, but did not affect the antimicrobial activity and mode of action. These results suggest that mBjAMP1 has a novel α-hairpinin-like scaffold and that mBjAMP1 and its analogs may be considered as useful templates for the development of peptide-based antibiotics.

■ RESULTS

Preparation of mBjAMP1 and Its Analogs. mBjAMP1 contains two cysteines in the primary sequence which form a single SS bond. Linear mBjAMP1 peptides were synthesized by solid-phase peptide synthesis (SPPS) of Fmoc chemistry with an amide resin (Table 1). The cysteine-reduced form of mBjAMP1 (mBjAMP1-re) was refolded into the cysteine-oxidized peptide (mBjAMP1-ox) to form an intramolecular SS bridge. Next, we designed two mBjAMP1 analogs to remove the SS bond, which are Cys-to-Ser substituted peptide (mBjAMP-ser) and Cys deleted peptide (mBjAMP1-del) to examine the structural and functional roles of the SS bond in mBjAMP1 (Table 1). The purity and molecular mass of the mBjAMP1 peptides were confirmed by analytical reversed phase-high performance liquid chromatography (RP-HPLC)
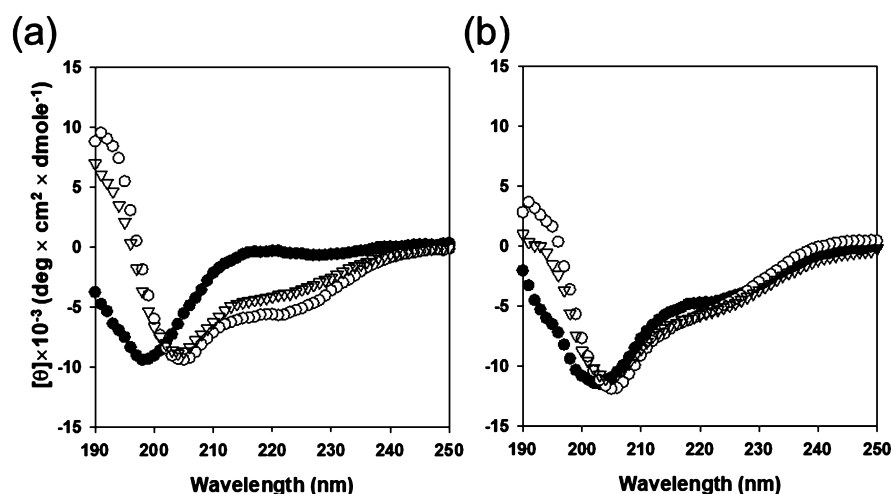
Figure 1. CD spectra of mBjAMP1-ser (a) and mBjAMP1-ox (b). The peptides were dissolved in 10 mM sodium phosphate (pH 7.0) (filled circles), 50% TFE (open circles), or 25 mM SDS (open triangles). The mean residue ellipticity was plotted against wavelength. The values from three scans were averaged per sample.

and liquid chromatography–mass spectrometry (LC–MS) analyses (all peptides above 95% pure; see Figure S1, Supporting Information). In addition, the N-terminal FITC-labeled mBjAMP1-ox and mBjAMP1-ser were synthesized to detect the localization of the peptides in bacterial and mammalian cells using confocal microscopy experiments.

Circular Dichroism (CD) Analysis. In order to analyze the structure of mBjAMP1 and its analogs, we measured the CD spectra of mBjAMP1-ser (a linear form without SS bond) and mBjAMP1-ox (a folded form with SS bond) under a variety of conditions, including 10 mM sodium phosphate buffer, 50% TFE solution, and 25 mM SDS micelles. mBjAMP1-ser showed a typical random coil CD spectrum having a negative minimum between 190 and 200 nm in 10 mM sodium phosphate buffer (Figure 1a). The random coil CD spectrum of mBjAMP1-ser was shifted to an α-helical CD characteristics with negative minima at 208 and 222 nm by adding TFE or SDS (Figure 1a). The CD spectrum of mBjAMP1-del also showed very similar characteristics as that of mBjAMP1-ser (Figure S2, Supporting Information). By contrast, the CD spectrum of mBjAMP1-ox was little changed by addition of TFE or SDS (Figure 1b). Interestingly, the CD spectrum of mBjAMP1-ox in 10 mM sodium phosphate buffer seems to be similar to that of mBjAMP1-ser in TFE or SDS buffer. The helix contents calculated from the CD data are summarized (Table S1, Supporting Information). The secondary structure of mBjAMP1-ser from CD spectrum in 10 mM sodium phosphate buffer could not be calculated due to the random coil characteristics. The helix content of mBjAMP1-ser was increased to around 18% by the addition of TFE or SDS. The helix content of mBjAMP1-ox was 15.6% even in sodium phosphate buffer without TFE or SDS. These data suggest that the helical conformation of mBjAMP1-ox is formed and stabilized by the intramolecular SS bond and is little affected by external buffer systems. To confirm that the SS bond can prevent unfolding of the mBjAM1, we performed the temperature scanning experiment for mBjAMP1-ox and mBjAMP1-ser in the presence of TFE using CD spectroscopy (Figure S3, Supporting Information). The CD spectra of mBjAMP1-ox were little changed by increasing temperature up to 60 °C (Figure S3a, Supporting Information). On the other hand, the CD spectra of mBjAMP1-ser were gradually shifted

by increasing temperature (Figure S3b, Supporting Information). We monitored the intensity at 222 nm which is one of the indicators of α-helical content (Figure S3c, Supporting Information). The CD intensities of mBjAMP1-ser were significantly decreasing by increasing temperature compared to those of mBjAMP1-ox. These data suggested that the SS bond of mBjAMP1-ox can prevent the unfolding of the mBjAMP1 peptide by heat denaturing condition.

Structure Calculation of mBjAMP1-ox. The NMR structure of mBjAMP1-ox was calculated using distance restraints obtained from nuclear Overhauser effect (NOE) constraints from 2D NOESY experiments[21,22] and SS bond connectivity (Table 2). The nearly complete ^{1}H resonance assignments for mBjAMP1-ox were performed by sequential NMR assignment procedure. The amino acid spin system was identified by the double quantum filtered COSY (DQF-COSY)[23] and total correlation spectroscopy (TOCSY)

Table 2. NMR Restraints and Structural Statistics for mBjAMP1-ox

| NMR restraints	no. of restraints
nuclear Overhauser effect (NOE)-derived distance restraints	241
disulfide bond restraints	3
structural statistics (20 structures)	
violations	
no. of distance restraints > 0.5 Å	0
RMSD from experiments	
distance (Å)	0.054 ± 0.009
RMSD from idealized geometry	
bonds (Å)	0.002 ± 0.001
angles (deg)	0.437 ± 0.018
impropers (deg)	0.290 ± 0.031
Ramachandran analysis (%) (all residues)	
most favored region	91.6
allowed region	7.1
disallowed region	7.3
average pairwise RMSD (Å) (residues 3–19)	
backbone heavy atoms	0.93 ± 0.24
all heavy atoms	1.78 ± 0.31
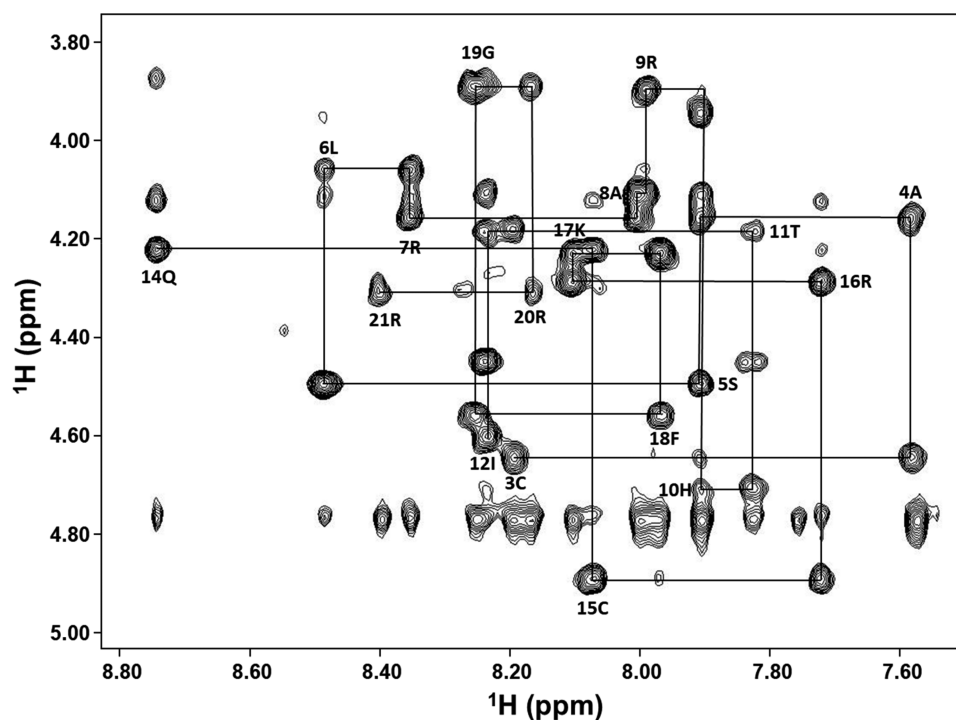
Figure 2. Sequential $d_{\alpha N}(i, i + 1)$ nuclear Overhauser effect (NOE) connectivities for mBjAMP1-ox in a ^{1}H 2D NOESY spectrum observed with a mixing time of 200 ms at 298 K. Intraresidue NH-C$^{\alpha}$H cross peaks are labeled with the residue number of mBjAMP1-ox using standard single-letter amino acid abbreviations. The first two residues (Asn1 and Leu2) and Pro13 of mBjAMP1-ox were not observed in the NOESY spectrum.

spectra.[24] The determined spin systems were ordered along the amino acid sequence of mBjAMP1-ox in the fingerprint region of the 2D NOESY spectrum including sequential $d_{\alpha N}(i, i +1)$ NOEs (Figure 2). Proton chemical shifts of mBjAMP1-ox are summarized (Table S2, Supporting Information). The 2D NOESY spectrum of mBjAMP1-ox showed all residues, except for the first two N-terminal residues (Asn1 and Leu2) and Pro13, and a good dispersion of cross peaks (Figure 2), indicating that mBjAMP1-ox has an ordered structural fold. By contrast, the random coil conformation of mBjAMP1-ser suggested by CD analysis was also confirmed by 2D NMR spectrum showing that the cross peaks of mBjAMP1-ser are not dispersed but gathered within the narrow range between 8.1 and 8.5 ppm (Figure S4, Supporting Information), indicating a disordered structure. The initial structure of mBjAMP1-ox was calculated using Cyana 2.1.[25] Next, the initial structures were refined using Xplor-NIH.[26] The final constraints and structural statistics for the mBjAMP1-ox are summarized (Table 2).

Structure Description of mBjAMP1-ox. The three-dimensional structure of mBjAMP1-ox determined by solution NMR spectroscopy is shown (Figure 3). Final 20 structures were well converged with root-mean-square deviation (RMSD) values of 0.93 ± 0.24 Å for backbone heavy atoms and 1.78 ± 0.31 Å for all heavy atoms in residues 3−19 (Figure 3a). The structure of mBjAMP1-ox is composed of two α-helices, consisting of residues 7−11(α1) and 14−19(α2) (Figure 3b). The two helices are connected by a short turn to produce a helix−turn−helix conformation. The N-terminal loop formed by residues 1−6 is connected to the α2 helix by the intramolecular SS bond between Cys3 and Cys15. The SS bond might stabilize the overall scaffold of mBjAMP1-ox since the structure of mBjAMP1 is disordered without the SS bond (Figure 1a). mBjAMP1 contains six positively charged residues

(five arginines and one lysine) that make mBjAMP1 highly positive. The positively charged residues except for Arg7 are located on one surface of the molecule, forming a large positive patch on the surface (Figure 3c and Figure 3d). Instead, all hydrophobic residues are placed on the other surface of the molecule. This residue distribution on the overall surface structure of mBjAMP1 induces amphipathic surface characteristics.

Antimicrobial Activity of mBjAMP1 Peptides. To examine the antimicrobial activity of mBjAMP1 peptides, we determined minimal inhibitory concentration (MIC) and minimal bactericidal concentration (MBC) values for mBjAMP1 and its analogs against three representative Gram-negative and three representative Gram-positive bacteria, as well as against several drug-resistant strains including MRSA, VRE, and MDRPA (Table 3 and Table S3, Supporting Information). The mBjAMP1 peptides showed broad antimicrobial activity with the MIC values within the range of 6.3− 12.5 μM. The MIC and MBC values of mBjAMP1-re and mBjAMP1-ox were identical. The antimicrobial activities of mBjAMP1-ser and mBjAMP1-del were slightly higher than those of mBjAMP1-re or mBjAMP1-ox based on GM values (12.5 vs 8.4 or 7.3 μM). All mBjAMP1 peptides also acted on drug-resistant strains with MIC values in the range of 12.5−50 μM. These results indicate that existence of the SS bond in mBjAMP1 may not affect the antimicrobial activity of mBjAMP1.

Time-Dependent Killing Kinetics. To study the association between the time of exposure to mBjAMP1 and bacterial survival, each of the representative species of Gram-negative (*E. coli*) and Gram-positive (*S. aureus*) bacteria was evaluated for exposure to mBjAMP1-ox and mBjAMP1-ser using the time−kill assay. When Gram-negative *E. coli* was exposed to 1 × MIC of the peptides, the bacterial survival was completely
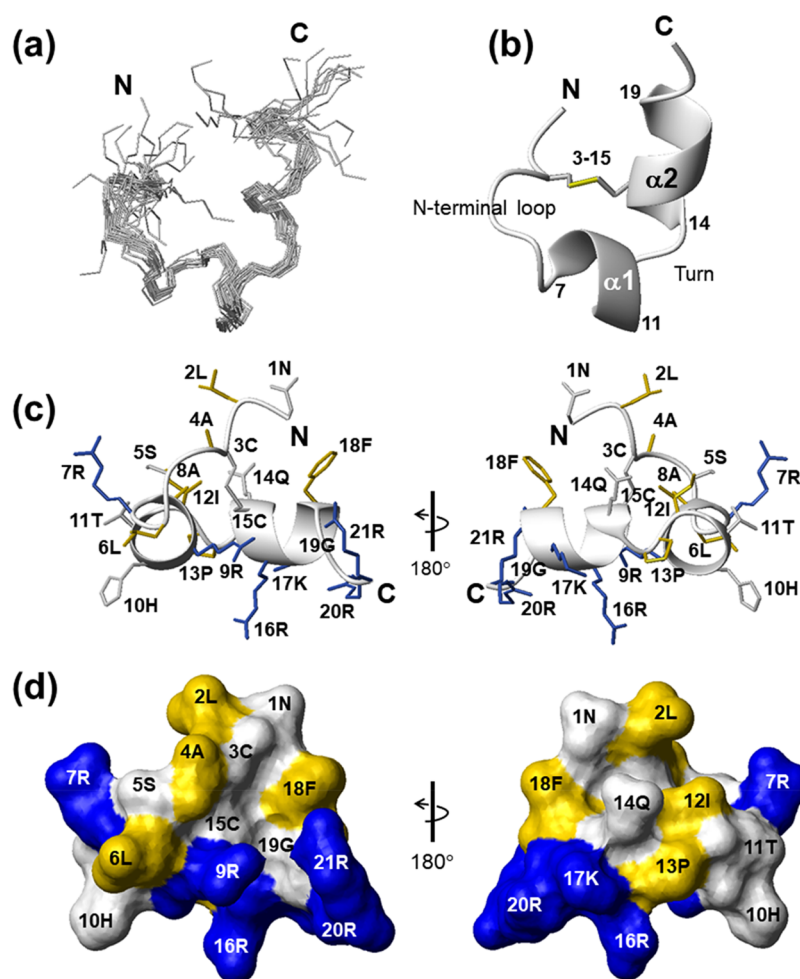
Figure 3. NMR solution structure of mBjAMP1-ox (PDB code 5Z1Y). (a) Twenty converged line structures of mBjAMP1-ox for backbone heavy atoms (N, C$^{\alpha}$, and C′). N and C indicate N- and C-terminal positions, respectively. (b) Lowest energy ribbon structure of mBjAMP1-ox. The α-helices (α1 and α2) are labeled and SS bonds are shown as a yellow stick. The N-terminal loop and turn are indicated. (c) Ribbon diagram with side chains of mBjAMP1-ox. (d) Surface structural characteristics of mBjAMP1-ox. All residues are labeled with their residue number and single-letter amino acid abbreviations. Positively charged and hydrophobic residues are indicated in blue and yellow, respectively.

reduced in 120−180 min (Figure 4). The survival of Gram-positive *S. aureus* was totally reduced in 30 min. The mBjAMP1-ox and mBjAMP1-ser showed a very similar manner, suggesting that the SS bond of mBjAMP1 does not affect killing kinetics of both Gram-negative and -positive bacteria. In addition, the number of cells showing fluorescence is much higher in *S. aureus* than in *E. coli* after 20 min incubation with FITC-labeled peptide (Figure S7a, Supporting Information), suggesting that mBjAMP1 peptide can penetrate *S. aureus* faster than *E. coli* cells. These results indicate that the bactericidal kinetics of mBjAMP1 peptides for Gram-positive is much faster than Gram-negative bacteria probably due to the extra outer membrane in Gram-negative bacteria.

Membrane Depolarization by mBjAMP1. To examine the mode of action of mBjAMP1 on the bacterial cytoplasmic membrane, we monitored membrane depolarization of mBjAMP1 peptides. The fluorescence intensity of DiSC3(5) was strongly quenched due to accumulation in the membrane (Figure 5a). After the signal remained stable for 200 s, mBjAMP1 peptides were added up to 8 × MIC (arrow). Similar to buforin II (well-known intracellular-targeting peptide) used as a negative control, all mBjAMP1 peptides (2 to 8 × MIC) did not induce any depolarization (Figure 5a

and Figure S5, Supporting Information). By contrast, melittin (well-known membrane-disrupting peptide) used as a positive control induced strong depolarization.

Membrane Permeabilization by mBjAMP1. To confirm membrane-targeting activity of mBjAMP1 peptides, SYTOX Green fluorescence, a DNA-binding dye, was used as a reporter to evaluate membrane permeabilization as well as formation of larger pores and holes in the bacterial membranes. SYTOX Green shows fluorescence when bound to nucleic acids. Similar to buforin II, mBjAMP1 peptides (2 to 8 × MIC) did not increase fluorescence intensity (Figure 5b and Figure S6, Supporting Information). By contrast, melittin induced the maximal fluorescence. Collectively, mBjAMP1 peptides did not affect the integrity of membrane structure but probably target intracellular components instead. Flow cytometry analysis was used to detect cell membrane integrity using propidium iodide (PI) staining of nucleic acids (Figure 6). The analysis revealed that the control without peptide resulted in only 2.36% PI positive cells. The percentage of PI-positive cells with membranes damaged by membrane-target control AMPs melittin and LL-37 was 55.50% and 75.38%, respectively, at 2 × MIC. By contrast, mBjAMP1-ox and mBjAMP1-ser exhibited either zero or low PI fluorescent signals of 6.39% and

Table 3. Minimal Inhibitory Concentration (MIC) of mBjAMP1 and Its Analogs against Gram-Negative, Gram-Positive, and Drug-Resistant Bacteria

| | peptide | | | | | | | |
| | mBjAMP-re | | mBjAMP-ox | | mBjAMP-ser | | mBjAMP-del | |
bacteria	(μM)	(μg/mL)	(μM)	(μg/mL)	(μM)	(μg/mL)	(μM)	(μg/mL)
Gram-negative								
Escherichia coli	12.5	31.0	12.5	31.0	6.3	15.4	6.3	14.3
Salmonella typhimurium	12.5	31.0	12.5	31.0	6.3	15.4	6.3	14.3
Pseudomonas aeruginosa	12.5	31.0	12.5	31.0	6.3	15.4	6.3	14.3
Gram-positive								
Bacillus subtilis	12.5	31.0	12.5	31.0	12.5	30.6	6.3	14.3
Staphylococcus aureus	12.5	31.0	12.5	31.0	12.5	30.6	12.5	28.5
Staphylococcus epidermidis	12.5	31.0	12.5	31.0	6.3	15.4	6.3	14.3
GM[a]	12.5	31.0	12.5	31.0	8.4	20.6	7.3	16.6
methicillin-resistant *Staphylococcus aureus*								
CCARM 3089	12.5	31.0	12.5	31.0	25.0	61.3	12.5	28.5
CCARM 3090	25.0	62.1	25.0	62.0	50.0	122.6	25.0	56.9
CCARM 3095	12.5	31.0	12.5	31.0	25.0	61.3	25.0	56.9
vancomycin-resistant *Enterococcus faecium*	25.0	62.1	25.0	62.0	50.0	>122.6	50.0	>113.9
multidrug-resistant *Pseudomonas aeruginosa*								
CCARM 2095	50.0	124.2	50.0	124.1	12.5	30.6	25.0	56.9

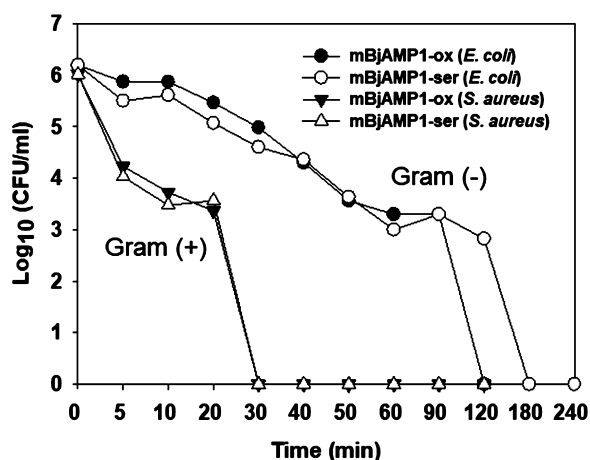[a]The geometric mean of MICs from six bacterial strains.

Figure 4. Time-dependent killing kinetics of mBjAMP1-ox and mBjAMP1-ser against Gram-negative *E. coli* and Gram-positive *S. aureus* with 1 × MIC peptides.

3.66%, respectively, at the same concentrations, which is similar to that of the intracellular-target AMP, buforin II (3.39%). These results suggest that the antimicrobial target of mBjAMP1-ox and mBjAMP1-ser is not the cytoplasmic membrane and also indicated that the SS bond in mBjAMP1 may not alter the mode of action of mBjAMP1 on the bacterial membrane.

Confocal Laser-Scanning Microscopy. In order to determine whether mBjAMP1 is able to penetrate bacterial cells without disrupting the cell membrane, FITC-labeled mBjAMP1-ox or FITC-labeled mBjAMP1-ser was incubated with representative species of Gram-negative *E. coli* and Gram-positive *S. aureus*. Localization of FITC-labeled mBjAMP1 peptides was visualized using confocal laser-scanning microscopy. Buforin II, used as a control, penetrated the bacterial cell membrane and accumulated in the cytoplasm of bacterial cells (Figure 7). Like buforin II, mBjAMP1-ox also entered the bacterial cell membrane of both *E. coli* and *S. aureus*. The mBjAMP1-ser showed results similar to that of mBjAMP1-ox

(Figure S7b, Supporting Information). On the other hand, the FITC-labeled mBjAMP1-ox likely binds on the surface of the mammalian cell membrane but does not fully penetrate the membrane, and then the peptide may be placed on the localized region of the mammalian cell (Figure S7c, Supporting Information). Therefore, it seems that mBjAMP1 peptide cannot penetrate into the nucleus to bind the mammalian DNA, and the cells survived. These results suggest that mBjAMP1 specifically affects the prokaryotes but not mammalian cells. To evaluate the influence of FITC fluorophore on the biological function of FITC-labeled mBjAMP1 peptide, we tested the antimicrobial activity of FITC-mBjAMP1-ox and FITC-mBjAMP1-ser. As a result, the antimicrobial activity of mBjAMP1-ox was not changed by FITC-labeling with 12.5 μM MIC against *E. coil* and *S. aureus* strain, and the antimicrobial activity of mBjAMP1-ser was slightly decreased by FITC-labeling (2- to 4-fold) (Figure S8a, Supporting Information).

DNA-Binding Activity. The mBjAMP1 peptide can inhibit bacterial growth by penetration of the bacterial cell membrane without causing cell disruption, suggesting that mBjAMP1 may target intracellular components. To test DNA binding ability of mBjAMP1, gel retardation assay was used with different amounts of mBjAMP1 peptide mixed with a plasmid DNA. Complete retardation of the DNA was observed at 32 μM for mBjAMP1-ox and 16 μM for mBjAMP1-ser (Figure 8). The buforin II as a control for DNA binding AMP also showed a complete retardation of the DNA at 32 μM concentration. The attachment of FITC fluorophore slightly affected to the DNA binding ability of mBjAMP1 peptides for full retardation (32 → 16 μM and 16 → 32 μM for mBjAMP1-ox and mBjAMP1-ser, respectively) (Figure S8b, Supporting Information).

Hemolytic Activity and Cytotoxicity. To evaluate bacterial cell selectivity of mBjAMP1 peptides, hemolytic activity against sheep red blood cell (sRBC) was measured in the range of 0.1−256 μM (Figure 9a). mBjAMP1 peptides produced almost no hemolysis (less than 1%) up to 256 μM. Melittin as the control peptide produced much higher
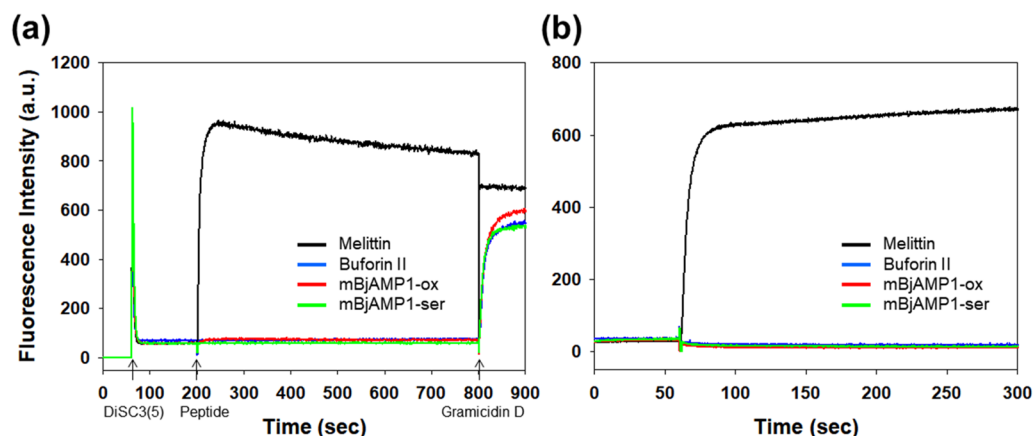
Figure 5. (a) Time-dependent depolarization of *S. aureus* cytoplasmic membrane induced by the peptides at 2 × MIC (melittin and buforin II) or 8 × MIC (mBjAMP1 peptides), determined using the membrane potential-sensitive fluorescence dye DiSC3(5). Dye release was monitored by measuring fluorescence. (b) Kinetics of *S. aureus* membrane permeabilization caused by peptides at 2 × MIC (melittin and buforin II) or 8 × MIC (mBjAMP1 peptides). Alterations of the cytoplasmic membrane allow the SYTOX Green probe to enter the cell and bind DNA, resulting in an increase of fluorescence.
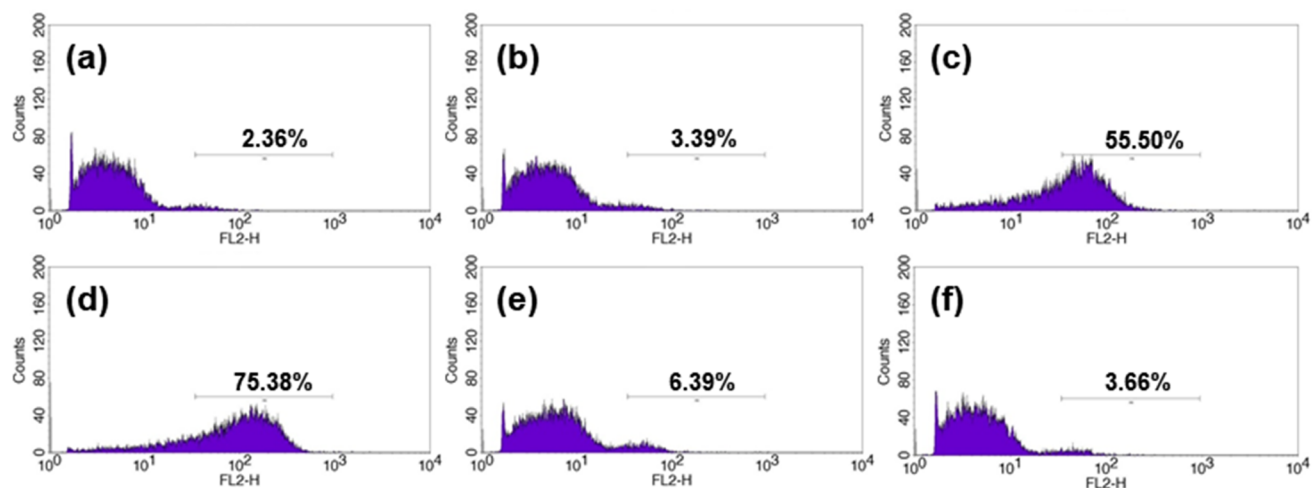

Figure 6. Flow cytometric analysis. Exponential-phase *E. coli* cells were treated with peptides, and cellular fluorescence was analyzed using flow cytometry. Increments of the log fluorescence signal represent PI uptake resulting from peptide treatment: (a) no peptide, negative control; (b) buforin II (2 × MIC, 16 μM); (c) melittin (2 × MIC, 4 μM); (d) LL-37 (2 × MIC, 16 μM); (e) mBjAMP1-ox (2 × MIC, 25 μM); (f) mBjAMP1-ser (2 × MIC, 12.5 μM).

hemolytic activity at a lower concentration (63% at 16 μM). Furthermore, we tested the cytotoxicity of mBjAMP1 peptides using MTT assay with RAW264.7 cells (Figure 9b). mBjAMP1-ox and mBjAMP1-ser showed very low cytotoxicity even at 512 μM. Melittin showed nearly 100% cytotoxicity from 32 μM onward.

■ DISCUSSION AND CONCLUSIONS

AMPs have attracted attention as a new class of antibiotics that may be useful in treating infectious diseases caused by antibiotic resistant bacteria. However, pharmaceutical use of AMPs has been hindered due to several factors, such as cytotoxicity to mammalian cells, low stability in vivo, and high cost of production.[27] Therefore, naturally constrained peptides, such as cysteine-rich peptides, are drawing much attention due to their excellent stability and pharmacokinetic properties.[28] For example, the cysteine-rich defensins play important roles in the innate immune system.[29] Defensins generally present a conserved cysteine-stabilized αβ (CSαβ) motif composed of an α-helix and two or three antiparallel β-strands stabilized

through two SS bridges.[30] Unlike better known cysteine-rich peptides such as defensins, mBjAMP1 possesses a distinct cysteine composition (only two cysteines within 21 amino acids exist) (Table 1), suggestive of a novel disulfide-stabilized AMP.[20] Two cysteines (Cys3 and Cys15) in mBjAMP1 were quickly oxidized to form a single intramolecular SS bond after air oxidation (Figure S1, Supporting Information). No dimer or oligomerization was found during the oxidative refolding procedure, suggesting that mBjAMP1 exists as a monomeric form with an intramolecular SS bond under oxidative conditions. mBjAMP1-ox was slightly eluted earlier than mBjAMP1-re on RP-HPLC (Figure S1, Supporting Information), probably because some hydrophobic residues were buried in the molecular core of mBjAMP1 and polar residues were exposed to solvent after SS bond formation.

To examine the structural role of the SS bond in mBjAMP1, we used CD spectra of mBjAMP1 peptides. CD analyses indicated that mBjAMP1-ox contains a helical structure, whereas mBjAMP1-ser and mBjAMP1-del were unstructured under aqueous conditions, but addition of TFE or SDS
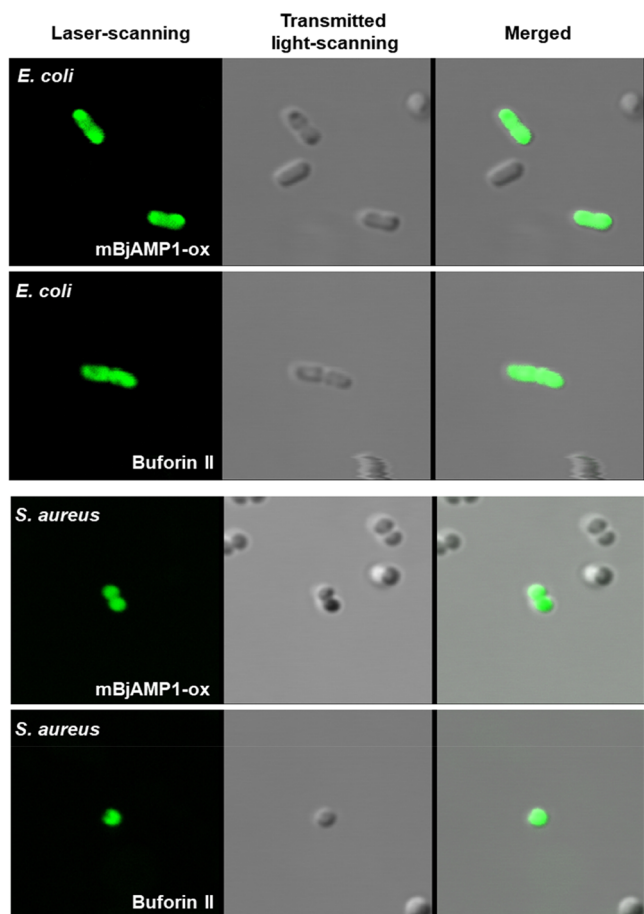
Figure 7. Localization of fluorescein isothiocyanate (FITC) labeled peptides on bacteria. Approximately 10^6 CFU/mL of *E. coli* or *S. aureus* cells were incubated with FITC labeled peptides. Bacteria were washed and fixed, and images were acquired using confocal microscopy.

Figure 9. (a) Hemolysis of sheep red blood cell by melittin (1−16 μM) and mBjAMP1 peptides (1−256 μM) and (b) cytotoxicity by MTT assay against mouse macrophage RAW 264.7 cells, induced by melittin or mBjAMP1 peptides (0−512 μM).

induced a helical conformation (Figure 1 and Figure S2, Supporting Information). The CD spectra of mBjAMP1-ox with or without TFE or SDS were very similar to each other and also similar to that of mBjAMP1-ser with TFE or SDS. TFE is a solvent that mimics the hydrophobic property of a microbial membrane, while SDS mimics a negatively charged bacterial membrane-comparable environment. These CD data indicated that the SS bond in mBjAMP1 may induce and stabilize the helical structure in mBjAMP1 without TFE or SDS.
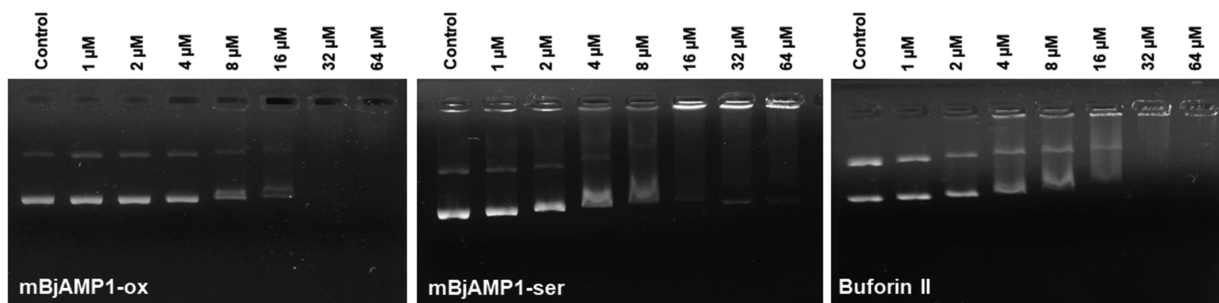
The NMR solution structure of mBjAMP1-ox revealed that mBjAMP1-ox is composed of two α-helices connected by a reverse turn, stabilized by an intramolecular SS bond (Figure 3). Recently, a novel helical hairpin fold stabilized by SS bonds was identified, based on the NMR structure of EcAMP-1 peptide purified from Barnyard grass.[31] The EcAMP-1 displays antifungal activity against several phytopathogenic fungi, and the structure of EcAMP-1 is composed of two α-helices connected by two SS bonds (Figure 10a). This peptide family, namely, α-hairpinin, has been acknowledged.[32] A typical

Figure 8. Interaction of peptides (mBjAMP1-ox, mBjAMP1-ser, or buforin II) with plasmid. Binding was assayed by measuring inhibition of migration by plasmid DNA (100 ng; pBR322). DNA and peptides (0−64 μM) were co-incubated for 1 h at room temperature before electrophoresis on a 1% agarose gel.
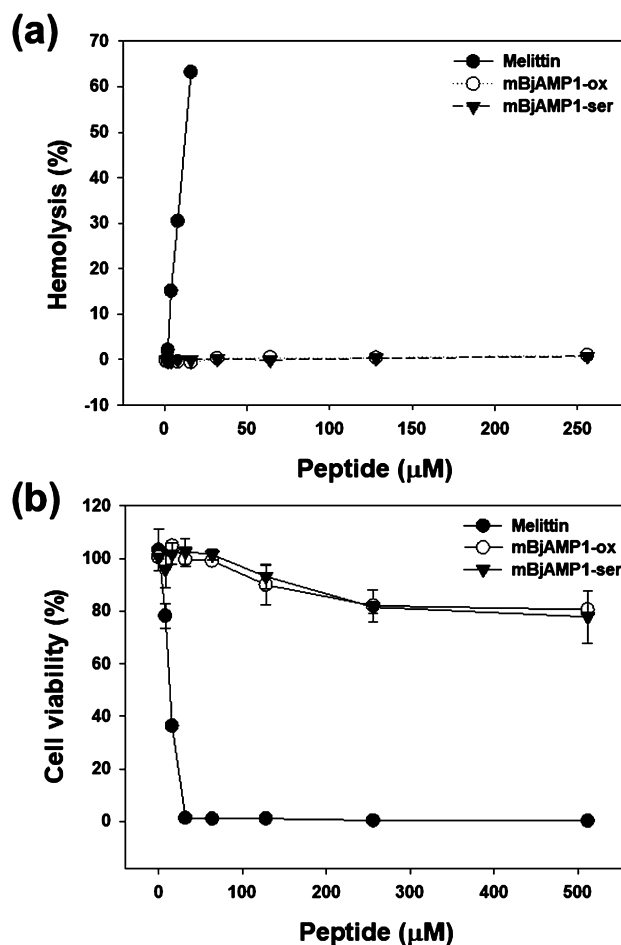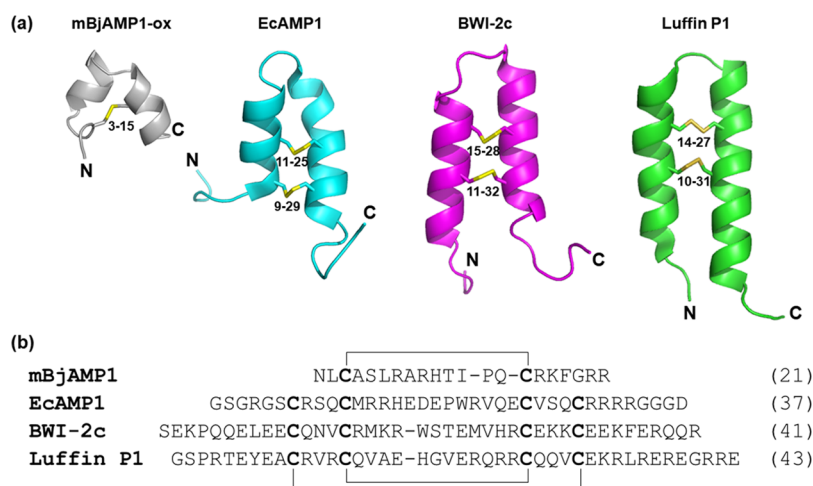
Figure 10. Structural comparison between mBjAMP1 and other α-hairpinins: (a) ribbon structures with SS bonds of mBjAMP1-ox, EcAMP1 (2L2R), BWI-2c (2LQX), and Luffin P1 (2L37); (b) sequence alignment of mBjAMP1 with other α-hairpinins. Cysteine residues are in bold. SS bonds are indicated by solid lines. The number of amino acids in each peptide is indicated in parentheses.

cysteine motif $C1X_3C2X_nC3X_3C4$, where X is any amino acid residue, characterizes α-hairpinin peptides. The α-hairpinin family includes peptides with diverse functions, such as antifungal activity, protein synthesis inhibition, and protease inhibition.[33] The α-hairpinin peptides consist of around 40 amino acids that form two antiparallel α-helices connected by two SS bonds. The overall fold of mBjAMP1 adopts α-hairpinin-like scaffold. However, the length of the primary sequence of mBjAMP1 is much shorter than those of α-hairpinins (Figure 10b), and mBjAMP1 has much shorter α-helices and only one SS bond compared to α-hairpinins. Although mBjAMP1 is much smaller than other α-hairpinins, mBjAMP1 displays an effective antimicrobial function.

For the highest antimicrobial activity and cell selectivity of AMPs, peptide molecules should have proper physicochemical properties such as the length of the sequence (12−16 amino acids) with positively charged (+5 to +7) and some hydrophobic residues which normally form an amphipathic helical structure for high antimicrobial activity.[34] Amphipathicity is generally considered to be crucial for the novel design and systematic optimization seen in α-helical AMPs.[35] mBjAMP1 appears to have an appropriate amino acid composition, with six positively charged and six hydrophobic residues, for antimicrobial activity. However, the helical wheel diagram of the primary sequence of mBjAMP1 peptides does not show amphipathic structural characteristics (Figure S9a, Supporting Information). Positively charged and hydrophobic residues are dispersed on the outer surface of the helix and do not form an amphipathic structure. The local region only in the second α-helix (α2) appears to exhibit rather amphipathic characteristics based on the helical wheel diagram (Figure S9b, Supporting Information). Interestingly, the surface profile of mBjAMP1-ox shows clear amphipathic surface characteristics (Figure 3d). The antimicrobial activity of mBjAMP1 may result from its overall surface profile which comprises amphipathic surface characteristics. The three-dimensional amphipathic arrangement of polar and hydrophobic residues in mBjAMP1 may provide it with the ability to interact with and permeabilize the bacterial membrane.

mBjAMP1-re appears to possess the same MIC values as mBjAMP1-ox. However, mBjAMP1-re, having two free cysteines, is easily oxidized in the neutral pH solution, and turns to mBjAMP1-ox, which makes it difficult to obtain exact MIC values of mBjAMP1-re. Therefore, to assess the functional role of the SS bond in mBjAMP1, we designed and synthesized two analogs without cysteines such as the Cys → Ser substitution (mBjAMP1-ser) and Cys deletion (mBjAMP1-del). These analogs showed similar or slightly higher antimicrobial activity compared to that of mBjAMP1-ox. These results indicated that the SS bond in mBjAMP1 is not critical for its antimicrobial activity. In fact, the effects of the SS bond on the activity of cysteine-rich AMPs varies depending on the AMP. For example, in the case of human β-defensin-1 (hBD-1), the antimicrobial activity is dramatically decreased by the SS bond, but human β-defensin-3 (hBD-3) retains the high antimicrobial activity regardless of the presence or absence of SS bonds.[36] In the case of mBjAMP1, the amino acid composition and sequence but not the SS bond may be critical for its antimicrobial activity.

To assess the antimicrobial mechanism of mBjAMP1, we first compared the time-dependent killing kinetics of Gram-negative (E. coli) and Gram-positive (S. aureus) bacteria. mBjAMP1 killed S. aureus more rapidly than E. coli (Figure 4). Gram-negative bacteria have additional outer membranes which are absent in Gram-positive bacteria, which result in various characteristics. For instance, Gram-negative bacteria are generally more resistant to antibiotics than Gram-positive bacteria, because the outer membrane of Gram-negative bacteria prevents efficient uptake of antibiotics. The time−killing assay using mBjAMP1 peptides also suggested that the membrane structures of bacteria may affect the bactericidal activity of mBjAMP1. Liu et al. suggested that mBjAMP1 may directly disrupt the bacterial membranes via a membranolytic mechanism.[20] Recently, Park et al. reported the mechanism of action of mBjAMP1 analog (IARR-Anal10) in which structural properties were changed by the addition of four amino acids (Ile-Ala-Arg-Arg) at the N-terminus rather than the native form of mBjAMP1. This IARR-Anal10 peptide increased α-helicity of the peptide by adding IARR sequence to the N-terminus and displayed more improved antimicrobial activity, as compared to native mBjAMP1. This IARR-Anal10 analog had little or no effect on bacterial outer membrane permeability or membrane integrity, but instead the analogs bind directly to bacterial DNA, suggesting IARR-Anal10 may

kill bacteria through intracellular targeting.[37] However, to date, the mechanism of action and structure–activity relationships of native mBjAMP1 have not been studied. We therefore investigated the mode of action of mBjAMP1 using various experimental approaches including membrane depolarization assay, SYTOX Green uptake assay, flow cytometry, confocal laser-scanning microscopy, and DNA binding assay. The results indicate that mBjAMP1 did not affect the integrity of bacterial membrane (Figures 5 and 6 and Figures S5 and S6, Supporting Information). Instead, mBjAMP1 is translocated to the interior of the bacterial cell (Figure 7 and Figure S7a, Supporting Information). Considered together, these results suggest that mBjAMP1 may be targeting intracellular components instead of the bacterial membrane to initiate their antimicrobial activity. Furthermore, as observed with buforin II, mBjAMP1 peptides directly interact with the bacterial DNA (Figure 8). DNA binding activity of mBjAMP1 was not affected by the presence of the SS bond. These results suggest that mBjAMP1 may target intracellular DNA or RNA to kill bacteria.

In conclusion, the detailed structural and functional assessment of mBjAMP1 peptides revealed that mBjAMP1 has a novel structural scaffold with broad antimicrobial activity through its cell permeability and DNA binding abilities. Cytotoxicity toward mammals displayed by AMPs is one of the major drawbacks to the use of AMPs as therapeutic agents. Fortunately, mBjAMP1 showed very low hemolysis and cytotoxicity to mammalian cells, suggesting that mBjAMP1 may be utilized as a structural template for the development of new peptide-based antibiotics.

■ EXPERIMENTAL SECTION

Materials. 9-Fluorenylmethoxycarbonyl (Fmoc) amino acids and amide resin were purchased from GL Biochem (China). All reagents including fluorescein isothiocyanate (FITC), diisopropylcarbodiimide (DIC), thioanisole (TIS), N,N-diisopropylethylamine (DIEA), ethanedithiol (EDT), 3-(4,5-dimethylthiazol-2-yl)-2,5-diphenyl-tetrazolium bromide (MTT), and trypsin (from bovine pancreas, EC 3.4.21.4) were supplied by Sigma-Aldrich (USA). We used total 13 microbial strains; three Gram-negative bacteria, three Gram-positive bacteria, and seven antibiotic-resistant bacteria (see Supporting Experimental 1 in Supporting Information for details).

Peptide Synthesis and Purification. The mBjAMP1 peptides were synthesized manually by SPPS using Fmoc chemistry (0.1 mmol scale) starting from MBHA-Rink amide resin (0.5–0.7 mmol/g loading). Fmoc from the resin was removed with 20% piperidine, wash resin with DMF, and swell resin with DCM. The coupling reaction of peptide bond was carried out for 120 min per coupling under the mixture of HOBt (2 equiv) and DIC (2 equiv) in DMF at 25 °C. For the FITC-labeled peptides, the Fmoc-ε-Ahx-OH was added to the N-terminus of the protected peptide during SPPS using standard coupling conditions. The final cleavage of the peptide from the resin and deprotection of amino acid side chain were carried out with a cocktail solution of TFA/TIS/phenol/H$_2$O/EDT (with a volume ratio of 82.5:5:5:5:2.5) for 3 h at 25 °C. The cleaved crude peptides were thoroughly washed with cold diethyl ether three times and were lyophilized. The linear peptides were purified using RP-HPLC (Shimadzu, Japan) on a Shim-pack C$_{18}$ column (20 mm × 250 mm, 5 μm particle size) monitored by UV detector (230 nm). The mobile phase components were 0.05% TFA in water (solvent A) and 0.05% TFA in acetonitrile (ACN) (solvent B). The purified products were confirmed by LC–MS analysis (API2000, AB SIEX, USA). The purity of the synthesized mBjAMP1 peptides was confirmed by analytical RP-HPLC (all peptides above 95% pure).

Oxidative Refolding. The linear mBjAMP1 (100 μM) was subjected to oxidative refolding to form SS bond in 50 mM sodium phosphate buffer (pH 7.5) with 30% ACN at 4 °C. Upon equilibrium, the reaction was quenched by acidification (pH 2.0) by adding TFA. The oxidative refolding of mBjAMP1 was monitored by RP-HPLC and LC–MS analysis.

CD Spectroscopy. Secondary structure of the mBjAMP1 peptides in 10 mM sodium phosphate buffer, 50% TFE solution, or 25 mM SDS micelles was characterized by CD spectroscopy. The CD spectra of the mBjAMP1 samples (100 μM) were measured using a J-815 CD spectropolarimeter (JASCO, Japan) in a quartz cell (1 mm path length). The spectra were averaged over three scans. The CD data were expressed as the mean residue ellipticity [θ] in degree square centimeter per decimole.

NMR Spectroscopy. NMR spectra were measured using a Bruker 600 MHz spectrometer. The NMR samples (2 mM mBjAMP1 peptides) used for NMR experiments were dissolved in in 10 mM sodium phosphate (pH 6.0) with 50 mM sodium chloride and 10% D$_2$O. 2D DQF-COSY, TOCSY, and NOESY spectra were collected at 298 K (see Supporting Experimental 2 in Supporting Information for details). 2D NMR data processing and analysis of mBjAMP1-ox were done using NMRPipe[38] and NMRView.[39]

Structure Calculation. The NOE peak assignments and NOE restraints of mBjAMP1-ox were obtained by Cyana 2.1.[40] All NOE restraints were manually refined during the Cyana structure calculations. The Cyana initial 100 structures were further refined using Xplor-NIH software with a simulated annealing protocol (see Supporting Experimental 3 in Supporting Information for details). The final 20 structures were chosen based on lowest energy for analysis, figure generation, and PDB deposition. All structure images were prepared with MOLMOL[41] and Pymol[42] program.

Determination of MIC and MBC. The MIC and MBC of mBjAMP1 peptides were examined in sterile 96-well 200 μL plates. An amount of 100 μL of bacterial cell suspension at 4 × 10^6 CFU/mL in 1% peptone was loaded to 100 μL of the sample solutions. After 18 h incubation at 37 °C, the MICs were defined by the lowest peptide concentration with no bacterial growth. Furthermore, MBCs were determined by removing 10 μL of MIC samples (at the end of incubation) from each well and plating onto LB agar plate. Colonies were counted after 18 h incubation at 37 °C. The MBC was defined as the lowest peptide concentration that killed greater than 99.9% of the initial inoculum.

Time-Dependent Killing Kinetics Assay. The time-dependent killing kinetics of the mBjAMP1 peptides was assessed using Gram-negative (E. coli) and Gram-positive (S. aureus) bacteria. Bacterial cells were cultured in LB media to mid log phase. The optical density at 600 nm (OD$_{600}$) of cells was adjusted to 0.5 (~10^6 CFU/mL) in 1% peptone. A final inoculum of 10^6 CFU/mL was treated with1 × MIC of mBjAMP1 peptides in 1% peptone. Aliquots were taken at 0–240 min and placed on LB agar plate and incubated for 18 h at 37 °C. After incubation, the colonies were counted. Each experiment was repeated independently on three separate days.

Membrane Depolarization Assay. To monitor the cytoplasmic membrane depolarization of bacterial cells, S. aureus was grown to the mid log phase (OD$_{600}$ = 0.5) and harvested by centrifugation. The cell pellet was washed two times with a sample buffer (20 mM glucose, 5 mM HEPES, and 10 mM KCl, pH 7.4) and diluted to 0.08 (OD$_{600}$) in the same buffer. The membrane potential-sensitive dye DiSC3(5) (20 nM) was mixed with the bacterial cell suspension and incubated until stable fluorescence reduction was achieved. The fluorescence intensity changes of DiSC3(5) were monitored using Shimadzu RF-5300PC fluorescence spectrophotometer (Shimadzu, Japan) (excitation = 622 nm, emission = 670 nm) after addition of mBjAMP1 (2, 4, and 8 × MIC) or control (2 × MIC) peptides. Gramicidin D (0.2 nM) was added to completely dissipate the membrane potential.

SYTOX Green Uptake Assay. S. aureus cells were cultured in LB broth to mid log phase at 37 °C and washed with the sample buffer (20 mM glucose, 5 mM HEPES, 10 mM KCl, pH 7.4) and resuspended (2 × 10^6 CFU/mL) in the same buffer. SYTOX Green dye (1 mM) was added to the bacterial suspension and incubated at 37 °C for 15 min with agitation in dark. Thereafter, mBjAMP1 peptides (2, 4, and 8 × MIC), buforin II (2 × MIC), or melittin (2 ×

MIC) was added, and then the increase in fluorescence was monitored using a Shimadzu RF-5300PC fluorescence spectrophotometer (Shimadzu, Japan) with an excitation wavelength of 485 nm and an emission wavelength of 520 nm.

Flow Cytometry. The bacterial membrane damage was confirmed by flow cytometry as previously described.[43] In brief, *E. coli* was grown to mid log phase in LB broth, washed three times with PBS, and diluted to 2×10^7 CFU/mL in PBS buffer. The peptides were incubated with the bacterial cell suspension and 10 μg/mL PI dye for 1 or 2 h at 37 °C, followed by washing the unbound dye with an excess of PBS buffer. The flow cytometry data were recorded using a FACScan instrument (FACSCalibur, Beckman Coulter Inc., USA) at an excitation wavelength of 488 nm.

Confocal Laser-Scanning Microscopy. *E. coli* and *S. aureus* cells were cultured in LB broth to mid log phase and harvested by centrifugation. The cell pellets were washed three times with PBS (pH 7.4) buffer. Bacteria (10^6 CFU/mL) cells or mammalian RAW 264.7 cells (Supporting Experimental 4 for mammalian cell culture, Supporting Information) were incubated with FITC-labeled peptides (30 μM) for 20 min at 37 °C. After incubation, the cells were harvested by centrifugation and then washed three times using PBS (pH 7.4) and fixed on a glass slide. The images of cells with FITC-labeled samples were collected using a Leica TCS SP5 confocal laser-scanning microscope (Leica Microsystems, Germany).

DNA-Binding Assay. We used gel retardation experiments to evaluate the ability of DNA binding of mBjAMP1 peptides. In brief, peptide samples were mixed with a fixed concentration (100 ng) of plasmid DNA (pBR322) in a sample buffer (10 mM Tris-HCl, 5% glucose, 50 μg/mL BSA, 1 mM EDTA, and 20 mM KCl). The mixture of DNA and peptide was incubated at 37 °C for 1 h. After incubation, the samples were analyzed by 1% agarose gel electrophoresis in 0.5% TAE buffer. The plasmid bands were detected by UV illuminator (Bio-Rad, USA).

Hemolytic Activity and MTT Assay. The hemolytic activity of mBjAMP1 peptides was determined by measuring the amount of free hemoglobin by the lysis of erythrocytes using sRBCs (see Supporting Experimental 5 in Supporting Information for details). The absorbance of hemoglobin was measured using a microplate ELISA reader (Bio-Tek Instruments EL800, USA) at 405 nm. To determine the cytotoxicity of the mBjAMP1 peptides, we used the MTT dye reduction assay against RAW 264.7 cells (see Supporting Experimental 5 in Supporting Information for details). In brief, the RAW 264.7 cells in 96-well plate were cultured for 24 h, and then mBjAMP1 peptide solutions were added and further incubated for 48 h. MTT solution (5 mg/mL) was added and further incubated for 4 h. After incubation, the precipitated MTT formazan crystal was dissolved by addition dimethyl sulfoxide (DMSO). Absorbance at 550 nm was measured using a microplate ELISA reader (Bio-Tek Instruments EL800, USA).

■ ASSOCIATED CONTENT

Ⓢ Supporting Information

The Supporting Information is available free of charge on the ACS Publications website at DOI: 10.1021/acs.jmedchem.8b01135.

> Prediction of helix contents from CD data; proton chemical shifts of mBjAMP1-ox; MIC and MBC of mBjAMP1 peptides; RP-HPLC and LC−MS analysis of mBjAMP1 peptides; CD spectra of mBjAMP1-ser and mBjAMP1-del; temperature scanning experiments for mBjAMP1 using CD spectroscopy; NOESY spectra of mBjAMP1-ox and mBjAMP1-ser; membrane depolarization of mBjAMP1 peptides; SYTOX Green uptake of mBjAMP1 peptides; confocal laser-scanning data of mBjAMP1-ser with *S. aureus* and mBjAMP1-ox with RAW 264.7 cells; MIC and DNA binding activity of FITC-labeled mBjAMP1-ox and -ser; helical wheel

> diagram of mBjAMP1 peptides; strains; NMR spectroscopy; structure calculation; mammalian cell cultures; hemolysis activity; MTT assay (PDF)
> Molecular formula strings and some data (CSV)

Accession Codes

PDB code for mBjAMP1-ox is 5Z1Y. Authors will release the atomic coordinates and experimental data upon article publication.

■ AUTHOR INFORMATION

Corresponding Authors

*S.Y.S.: phone, +82-62-230-6769; e-mail, syshin@chosun.ac.kr.
*C.W.L.: phone, +82-62-530-3374; e-mail, cwlee@jnu.ac.kr.

ORCID ⊙

Song Yub Shin: 0000-0002-3030-7973
Chul Won Lee: 0000-0002-3205-675X

Author Contributions

J.N., H.Y., G.R., and S.D.K. conducted the experiments. J.I.K., H.J.M., S.Y.S., and C.W.L. designed the experiments. J.N., S.Y.S., and C.W.L. wrote the manuscript. All authors read and approved the final manuscript.

Notes

The authors declare no competing financial interest.

■ ABBREVIATIONS USED

ACN, acetonitrile; AMP, antimicrobial peptide; ATCC, American Type Culture Collection; CCARM, Culture Collection of Antimicrobial Resistant Microbes; CS$\alpha\beta$, structural cysteine-stabilized $\alpha\beta$; DIC, diisopropylcarbodiimide; DIEA, *N,N*-diisopropylethylamine; DMEM, Dulbecco's modified Eagle medium; DMF, *N,N*-dimethylformamide; DQF-COSY, double quantum filtered correlation spectroscopy; EDT, ethanedithiol; FBS, fetal bovine serum; FITC, fluorescein isothiocyanate; GM, geometric mean of minimal inhibitory concentrations; hBD, human β-defensin; HOBt, 1-hydroxybenzotriazole; KCTC, Korean Collection for Type Cultures; LB, Luria−Bertani; MBC, minimal bactericidal concentration; MDR, multidrug resistant; MTT, 3-(4,5-dimethylthiazol-2-yl)-2,5-diphenyltetrazolium bromide; PI, propidium iodide; SPPS, solid-phase peptide synthesis; SS, disulfide; TFE, 2,2,2-trifluoroethanol; TIS, thioanisole; TOCSY, total correlation spectroscopy

■ REFERENCES

(1) Frieri, M.; Kumar, K.; Boutin, A. Antibiotic resistance. *J. Infect Public Health* **2017**, *10*, 369−378.
(2) Roca, I.; Akova, M.; Baquero, F.; Carlet, J.; Cavaleri, M.; Coenen, S.; Cohen, J.; Findlay, D.; Gyssens, I.; Heure, O. E.; Kahlmeter, G.; Kruse, H.; Laxminarayan, R.; Liebana, E.; Lopez-Cerero, L.; MacGowan, A.; Martins, M.; Rodriguez-Bano, J.; Rolain, J. M.; Segovia, C.; Sigauque, B.; Tacconelli, E.; Wellington, E.; Vila, J. The global threat of antimicrobial resistance: science for intervention. *New Microbes New Infect.* **2015**, *6*, 22−29.

(3) Hale, J. D.; Hancock, R. E. Alternative mechanisms of action of cationic antimicrobial peptides on bacteria. *Expert Rev. Anti-Infect. Ther.* 2007, 5, 951–959.

(4) Seo, M. D.; Won, H. S.; Kim, J. H.; Mishig-Ochir, T.; Lee, B. J. Antimicrobial peptides for therapeutic applications: a review. *Molecules* 2012, 17, 12276–12286.

(5) Tossi, A.; Sandri, L.; Giangaspero, A. Amphipathic, alpha-helical antimicrobial peptides. *Biopolymers* 2000, 55, 4–30.

(6) Lehrer, R. I.; Ganz, T. Antimicrobial peptides in mammalian and insect host defence. *Curr. Opin. Immunol.* 1999, 11, 23–27.

(7) Melo, M. N.; Ferre, R.; Castanho, M. A. Antimicrobial peptides: linking partition, activity and high membrane-bound concentrations. *Nat. Rev. Microbiol.* 2009, 7, 245–250.

(8) Hurdle, J. G.; O'Neill, A. J.; Chopra, I.; Lee, R. E. Targeting bacterial membrane function: an underexploited mechanism for treating persistent infections. *Nat. Rev. Microbiol.* 2011, 9, 62–75.

(9) Zhang, L. J.; Gallo, R. L. Antimicrobial peptides. *Curr. Biol.* 2016, 26, R14–19.

(10) Hancock, R. E.; Lehrer, R. Cationic peptides: a new source of antibiotics. *Trends Biotechnol.* 1998, 16, 82–88.

(11) Wimley, W. C. Describing the mechanism of antimicrobial peptide action with the interfacial activity model. *ACS Chem. Biol.* 2010, 5, 905–917.

(12) Nguyen, L. T.; Haney, E. F.; Vogel, H. J. The expanding scope of antimicrobial peptide structures and their modes of action. *Trends Biotechnol.* 2011, 29, 464–472.

(13) Seefeldt, A. C.; Graf, M.; Perebaskine, N.; Nguyen, F.; Arenz, S.; Mardirossian, M.; Scocchi, M.; Wilson, D. N.; Innis, C. A. Structure of the mammalian antimicrobial peptide Bac7(1–16) bound within the exit tunnel of a bacterial ribosome. *Nucleic Acids Res.* 2016, 44, 2429–2438.

(14) Roy, R. N.; Lomakin, I. B.; Gagnon, M. G.; Steitz, T. A. The mechanism of inhibition of protein synthesis by the proline-rich peptide oncocin. *Nat. Struct. Mol. Biol.* 2015, 22, 466–469.

(15) Li, W. F.; Ma, G. X.; Zhou, X. X. Apidaecin-type peptides: biodiversity, structure-function relationships and mode of action. *Peptides* 2006, 27, 2350–2359.

(16) Hsu, C. H.; Chen, C.; Jou, M. L.; Lee, A. Y.; Lin, Y. C.; Yu, Y. P.; Huang, W. T.; Wu, S. H. Structural and DNA-binding studies on the bovine antimicrobial peptide, indolicidin: evidence for multiple conformations involved in binding to membranes and DNA. *Nucleic Acids Res.* 2005, 33, 4053–4064.

(17) Boman, H. G.; Agerberth, B.; Boman, A. Mechanisms of action on Escherichia coli of cecropin P1 and PR-39, two antibacterial peptides from pig intestine. *Infect. Immun.* 1993, 61, 2978–2984.

(18) Park, C. B.; Yi, K. S.; Matsuzaki, K.; Kim, M. S.; Kim, S. C. Structure-activity analysis of buforin II, a histone H2A-derived antimicrobial peptide: the proline hinge is responsible for the cell-penetrating ability of buforin II. *Proc. Natl. Acad. Sci. U. S. A.* 2000, 97, 8245–8250.

(19) Park, C. B.; Kim, H. S.; Kim, S. C. Mechanism of action of the antimicrobial peptide buforin II: buforin II kills microorganisms by penetrating the cell membrane and inhibiting cellular functions. *Biochem. Biophys. Res. Commun.* 1998, 244, 253–257.

(20) Liu, H.; Lei, M.; Du, X.; Cui, P.; Zhang, S. Identification of a novel antimicrobial peptide from amphioxus *Branchiostoma japonicum* by in silico and functional analyses. *Sci. Rep.* 2016, 5, 18355.

(21) Macura, S.; Huang, Y.; Suter, D.; Ernst, R. R. Two-dimensional chemical exchange and cross-relaxation spectroscopy of coupled nuclear spins. *J. Magn. Reson.* 1981, 43, 259–281.

(22) Jeener, J.; Meier, B. H.; Bachmann, P.; Ernst, R. R. Investigation of exchange processes by two-dimensional NMR spectroscopy. *J. Chem. Phys.* 1979, 71, 4546–4553.

(23) Rance, M.; Sorensen, O. W.; Bodenhausen, G.; Wagner, G.; Ernst, R. R.; Wuthrich, K. Improved spectral resolution in cosy 1H NMR spectra of proteins via double quantum filtering. *Biochem. Biophys. Res. Commun.* 1983, 117, 479–485.

(24) Bax, A.; Davis, D. G. MLEV-17-based two-dimensional homonuclear magnetization transfer spectroscopy. *J. Magn. Reson.* 1985, 65, 355–360.

(25) Guntert, P. Automated NMR structure calculation with CYANA. *Methods Mol. Biol.* 2004, 278, 353–378.

(26) Schwieters, C. D.; Kuszewski, J. J.; Tjandra, N.; Clore, G. M. The Xplor-NIH NMR molecular structure determination package. *J. Magn. Reson.* 2003, 160, 65–73.

(27) Aoki, W.; Ueda, M. Characterization of antimicrobial peptides toward the development of novel antibiotics. *Pharmaceuticals* 2013, 6, 1055–1081.

(28) Gongora-Benitez, M.; Tulla-Puche, J.; Albericio, F. Multi-faceted roles of disulfide bonds. Peptides as therapeutics. *Chem. Rev.* 2014, 114, 901–926.

(29) Hazlett, L.; Wu, M. Defensins in innate immunity. *Cell Tissue Res.* 2011, 343, 175–188.

(30) de Oliveira Dias, R.; Franco, O. L. Cysteine-stabilized alphabeta defensins: From a common fold to antibacterial activity. *Peptides* 2015, 72, 64–72.

(31) Nolde, S. B.; Vassilevski, A. A.; Rogozhin, E. A.; Barinov, N. A.; Balashova, T. A.; Samsonova, O. V.; Baranov, Y. V.; Feofanov, A. V.; Egorov, T. A.; Arseniev, A. S.; Grishin, E. V. Disulfide-stabilized helical hairpin structure and activity of a novel antifungal peptide EcAMP1 from seeds of barnyard grass (*Echinochloa crus-galli*). *J. Biol. Chem.* 2011, 286, 25145–25153.

(32) Oparin, P. B.; Mineev, K. S.; Dunaevsky, Y. E.; Arseniev, A. S.; Belozersky, M. A.; Grishin, E. V.; Egorov, T. A.; Vassilevski, A. A. Buckwheat trypsin inhibitor with helical hairpin structure belongs to a new family of plant defence peptides. *Biochem. J.* 2012, 446, 69–77.

(33) Slavokhotova, A. A.; Rogozhin, E. A.; Musolyamov, A. K.; Andreev, Y. A.; Oparin, P. B.; Berkut, A. A.; Vassilevski, A. A.; Egorov, T. A.; Grishin, E. V.; Odintsova, T. I. Novel antifungal alpha-hairpinin peptide from Stellaria media seeds: structure, biosynthesis, gene structure and evolution. *Plant Mol. Biol.* 2014, 84, 189–202.

(34) Jiang, Z.; Vasil, A. I.; Hale, J.; Hancock, R. E.; Vasil, M. L.; Hodges, R. S. Effects of net charge and the number of positively charged residues on the biological activity of amphipathic alpha-helical cationic antimicrobial peptides. *Adv. Exp. Med. Biol.* 2009, 611, 561–562.

(35) Zhu, X.; Dong, N.; Wang, Z.; Ma, Z.; Zhang, L.; Ma, Q.; Shan, A. Design of imperfectly amphipathic alpha-helical antimicrobial peptides with enhanced cell selectivity. *Acta Biomater.* 2014, 10, 244–257.

(36) Schroeder, B. O.; Wu, Z.; Nuding, S.; Groscurth, S.; Marcinowski, M.; Beisner, J.; Buchner, J.; Schaller, M.; Stange, E. F.; Wehkamp, J. Reduction of disulphide bonds unmasks potent antimicrobial activity of human beta-defensin 1. *Nature* 2011, 469, 419–423.

(37) Park, J.; Kang, H. K.; Choi, M. C.; Chae, J. D.; Son, B. K.; Chong, Y. P.; Seo, C. H.; Park, Y. Antibacterial activity and mechanism of action of analogues derived from the antimicrobial peptide mBjAMP1 isolated from Branchiostoma japonicum. *J. Antimicrob. Chemother.* 2018, 73, 2054–2063.

(38) Delaglio, F.; Grzesiek, S.; Vuister, G. W.; Zhu, G.; Pfeifer, J.; Bax, A. NMRPipe: a multidimensional spectral processing system based on UNIX pipes. *J. Biomol. NMR* 1995, 6, 277–293.

(39) Johnson, B. A.; Blevins, R. A. NMR View: A computer program for the visualization and analysis of NMR data. *J. Biomol. NMR* 1994, 4, 603–614.

(40) Herrmann, T.; Guntert, P.; Wuthrich, K. Protein NMR structure determination with automated NOE assignment using the new software CANDID and the torsion angle dynamics algorithm DYANA. *J. Mol. Biol.* 2002, 319, 209–227.

(41) Koradi, R.; Billeter, M.; Wuthrich, K. MOLMOL: a program for display and analysis of macromolecular structures. *J. Mol. Graphics* 1996, 14, 51–55.

(42) *The PyMOL Molecular Graphics System*, version 1.8; Schrodinger, LLC.

(43) Dong, N.; Ma, Q.; Shan, A.; Lv, Y.; Hu, W.; Gu, Y.; Li, Y. Strand length-dependent antimicrobial activity and membrane-active mechanism of arginine- and valine-rich beta-hairpin-like antimicrobial peptides. *Antimicrob. Agents Chemother.* **2012**, *56*, 2994−3003.